

Normal-Mode Analysis of Circular DNA at the Base-Pair Level. 1. Comparison of Computed Motions with the Predicted Behavior of an Ideal Elastic Rod

Atsushi Matsumoto,^{†,‡} Irwin Tobias,[†] and Wilma K. Olson^{*,†}

Department of Chemistry and Chemical Biology, Rutgers, The State University of New Jersey, Wright-Rieman Laboratories, 610 Taylor Road, Piscataway, New Jersey 08854-8087, and Quantum Bioinformatics Group, Center for Promotion of Computational Science and Engineering, Japan Atomic Energy Research Institute, 8-1 Umemidai, Kizu, Kyoto 619-0215, Japan

Received August 31, 2004

Abstract: We have extended a newly developed approach to study the low-frequency normal modes of mesoscopic fragments of linear DNA in order to investigate the dynamics of closed circular molecules of comparable size, i.e., a few hundred base pairs. We have added restraint energy terms and a global minimization step to treat the more complicated, spatially constrained duplex in terms of the intrinsic conformation and flexibility of the constituent base-pair “step” parameters. Initial application of the methodology to the normal modes of an ideal closed circular DNA molecule—which is naturally straight in its relaxed open linear state, inextensible, and capable of isotropic bending and independent twisting at the base-pair level—matches theoretical predictions of elastic rod dynamics. The energy-optimized closed circular states and the types of low frequency motions follow expected behavior, with (1) uniform twist density and uniform energy density in the minimum energy state; (2) a near-zero frequency torsional mode with “free” rotation about the global helical axis; (3) higher-order torsional modes accompanied by global rocking motions and pure in-plane and out-of-plane bending motions in the torsionally relaxed circle; and (4) mixed modes of bending when the chain is supercoiled (over- or undertwisted). Furthermore, the computed changes in normal-mode frequencies with imposed supercoiling or with variation of chain length are virtually identical to theoretically predicted values.

Introduction

The elastic properties of DNA are revealed in its dynamic structure. Experiments that probe the dynamics of DNA are usually interpreted in terms of the motions of a spatially homogeneous, naturally straight, elastic rod without distinguishing chemical features, and any local sequence-dependent behavior is folded into three global constants tied to the overall bending, twisting, and stretching of the molecule. By contrast, computations of the dynamics of DNA are often highly detailed, allowing for the movement of each atom in the double helical structure and the surrounding layers of

solvent. The level of detail in such studies precludes the simulation of mesoscopic pieces of DNA of a few hundred base pairs, and conversely, computational treatment of mesoscopic DNA fragments necessitates some loss of information about chemical fine structure.

Recently, we reported a new computational approach for studying the dynamic properties of relatively long, linear DNA molecules without losing track of the local conformational features.¹ Specifically, we identify the low frequency normal modes that underlie the global bending, twisting, and stretching of defined polymeric sequences. Application of the method to representative DNA chain models reveals subtle relationships between sequence and collective polymeric motions. For example, the appropriate spacing of highly deformable pyrimidine-purine dimer steps in phase

* Corresponding author phone: (732)445-3993; fax: (732)445-5958; e-mail: olson@rutchem.rutgers.edu.

[†] Rutgers, The State University of New Jersey.

[‡] Japan Atomic Energy Research Institute.

with the 10-fold double helical repeat induces a mesoscopic bending anisotropy that is conducive to DNA loop formation.

The computations have now been extended so that it is possible to study more complicated DNA systems, where the structure of the double helix is restrained by long-range physical or chemical forces. In this paper, we report the dynamic properties of closed circular DNA, one of the simplest systems that can be studied with the new approach. We compare our numerical results with the theoretically predicted dynamical properties of a circular DNA modeled as an ideal, inextensible elastic rod.

Methods

We take advantage of a newly developed computational method for carrying out normal-mode analyses of long, linear DNA molecules in terms of the constituent base-pair step parameters.¹ The approach taken here is identical in all respects to the earlier work, except for an additional energy term needed to keep the ends of the chain in place and an initial energy minimization step used to incorporate this anchoring constraint. We thus omit further description of the methodology and refer the reader to the literature¹ for additional information. We focus instead on the independent variables and potential function used in the present calculations, the energy minimization process, and the theoretical principles used to determine the normal modes of DNA.

Independent Variables. Normal-mode analyses of proteins and nucleic acids are usually performed in Cartesian or dihedral angle space. The set of individual atomic coordinates used to specify molecular structure in the former case has two important computational advantages: (1) the simple form of the equations of molecular motion and (2) the detailed information about local conformational change that can be obtained from the analysis. The applicability of Cartesian-based studies is limited, however, by the large number of variables needed to describe molecular structure. The use of dihedral angles as independent variables partially overcomes this limitation, with a reduction in the number of conformational parameters realized by setting the chemical bond lengths and valence angles to equilibrium values and taking only the rotatable dihedral angles as independent variables. The contribution of the latter parameters to overall polymeric motions is dominant even if all chemical degrees of freedom are considered. Therefore, as long as one is interested in the global properties of a macromolecule, normal-mode analysis in dihedral angle space can be quite effective.^{2–4}

In the case of nucleic acids, there is an even simpler way to describe three-dimensional molecular motion. Because each base or base pair can be approximated as a rigid body, molecular structure can be described in terms of the relative positions and orientations of complementary bases or successive base pairs. Six rigid-body parameters are needed to specify the relative position of each pair of rigid bodies. In this study, we treat the base pairs as rigid objects and use the six base-pair step parameters—Tilt, Roll, Twist, Shift, Slide, Rise⁵—as independent variables. The description of nucleic acid structure is not complete, however, without specification of the sugar–phosphate backbone. We therefore

treat each DNA strand as a chain of nucleotide 5′-monophosphates, with each residue fixed in the B-form and related to its sequential neighbors by a given set of local base-pair step parameters. This treatment drastically reduces the number of variables needed to describe helical structure and is key to the present study of mesoscopic-length DNA circles. The step parameters are defined according to the formulation of El Hassan and Calladine,⁶ and the backbone is incorporated by superposition of a 5′-nucleotide fragment from the canonical B-DNA fiber diffraction model.⁷ The local chemical environment is implicitly treated in terms of the range of allowed dimeric deformations (see below). The ensemble properties deduced from the normal modes are independent of the surrounding medium, e.g., solvent viscosity.

Force Field. Minimization of the potential energy is carried out prior to normal-mode analysis and is the most time-consuming part of the calculation. The simple form of the energy, made up of the internal dimer step energies and an external ring-closure restraint term, accelerates the energy minimization step.

The energy of each dimer step, E_d , is expressed as a sum of elastic contributions over the six base-pair step parameters⁸

$$E_d = \frac{1}{2} \sum_{i=1}^6 \sum_{j=1}^6 f_{ij} (\theta_i - \theta_i^u) (\theta_j - \theta_j^u) \quad (1)$$

where the θ_i ($i = 1, 2, \dots, 6$) are the instantaneous values of the base-pair step parameters—Tilt, Roll, Twist, Shift, Slide, Rise—of a given dinucleotide step and the θ_i^u are the equilibrium values of the parameters in an undeformed, linear B-DNA reference state. The total internal energy is a sum of the E_d values for the n_B base-pair steps of the cyclic molecule. Here, to facilitate comparison of the computed normal modes with the theoretically predicted fluctuations of an elastic rod, we consider an ideal, naturally straight B-DNA homopolymer in which each dimer adopts an identical equilibrium rest state. In this model, the planes of neighboring base pairs are perfectly parallel ($\theta_1^u = \theta_2^u = 0^\circ$), the equilibrium Twist is fixed at $\theta_3^u = 36^\circ$, and the sequential displacement is restricted to Rise, i.e., $\theta_4^u = \theta_5^u = 0 \text{ \AA}$; $\theta_6^u = 3.4 \text{ \AA}$.

The elastic constants in eq 1, f_{ij} , are similarly chosen to mimic the known properties of an ideal rod. The variation of individual “step” parameters is thus assumed to be independent of one another, and the f_{ij} of cross terms ($i \neq j$) are set equal to zero. As a result, only self-product terms remain in eq 1. An energy of $k_B T/2$ is assigned to each such term at thermal equilibrium. Thus, the elastic constants f_{ii} are described in terms of the mean-square fluctuations, i.e., $f_{ii} = k_B T / \langle \Delta \theta_i^2 \rangle$, where k_B is the Boltzmann constant and T the temperature in Kelvin. The expression of the f_{ii} in this form is convenient for calibrating equilibrium properties of the DNA model,⁹ including the persistence length, a measure of the distance over which segments of the polymer remain directionally correlated.¹⁰ [The scaling of the local energy in terms of the thermal fluctuations of individual base-pair step parameters should not be confused with the normal mode deformations of the DNA as a whole, which are described below in terms of global energy changes of $k_B T/2$ or less.] The energy change in the sugar–phosphate back-

bone associated with the variation of base-pair step parameters is implicitly considered in the potential, validating the incorporation of fixed backbone units noted above. Bending deformations are assumed to be isotropic and are calibrated such that the persistence length of the linear chain is 500 Å,⁹ i.e., $\langle \Delta \text{Tilt}^2 \rangle^{1/2} = \langle \Delta \text{Roll}^2 \rangle^{1/2} = 4.7^\circ$. The variation in dimeric twist, $\langle \Delta \text{Twist}^2 \rangle^{1/2}$, is set to 4° based on estimates of the fluctuations of helical twist in supercoiled DNA involving considerations of the residual writhe in closed circular structures.^{11–13} The force constants of the displacement variables— $\langle \Delta \text{Shift}^2 \rangle^{1/2} = \langle \Delta \text{Slide}^2 \rangle^{1/2} = \langle \Delta \text{Rise}^2 \rangle^{1/2} = 0.1$ Å—are assigned values large enough to preclude stretching so that the model is directly comparable to the representation of DNA used in the theory of an ideal inextensible elastic rod.^{14,15} Calculations based on the model can thus be compared with predictions of the theory. The choice of local force constants produces a linear polymer with global elastic properties characterized by a bending rigidity A of 2.1×10^{-19} erg-cm and a twisting modulus C of 2.9×10^{-19} erg-cm. The latter values are obtained from the computed normal-mode frequencies of the linear molecule.¹ Effects of sequence, i.e., the known sequence-dependent fine structure and deformability of DNA,⁸ are not considered in the theory and are thus ignored in the present calculations. The assumed DNA variability is, nevertheless, comparable to the range of conformational distortions seen in high-resolution crystal structures but is broader than the local angular fluctuations deduced from direct measurements of short-time chain dynamics.^{16,17} As discussed previously,¹ the potential energy of DNA is not a smooth quadratic function. Whereas the equilibrium bending properties of DNA reflect transitions between multiple discrete minima, the apparent stiffness of the DNA probed in the time-dependent experiments seemingly arises from molecules trapped in a single low-energy state.

The restraint energy, E_r , is given by a sum over N distance restraints

$$E_r = \sum_{k=1}^N C_k (d_k - d_k^0)^2 \quad (2)$$

where C_k is an arbitrarily chosen spring constant, d_k is the instantaneous distance between two points on which a distance restraint is placed, and d_k^0 is the desired separation distance. Restraints that force the overlap of the origins and the x - and z -axes of terminal base pairs are used to generate DNA circles. Because the restraint energy is close to zero after energy minimization, the dimeric contributions from eq 1 dominate the total energy.

Energy Minimization. The normal modes of a molecule are collective, low-energy motions of the system as a whole in the vicinity of its minimum energy configuration. The deformations in global structure are described by harmonic fluctuations of individual conformational parameters from their rest values at the energy minimum. In the case of linear DNA, the minimum energy state is self-evident from the equilibrium rest states, i.e., θ_i^0 values, of sequential dimers. The minimum energy configuration of circular DNA, however, cannot be determined a priori because of the additional

long-range distance restraint(s). Therefore, numerical calculations must be performed to find the state of lowest energy. Both conjugate gradient and Newton–Raphson methods are used in the minimization process, the former approach introduced at the first stage of optimization and the latter technique once the decrease of energy per iteration becomes small. Determination of the requisite first and second derivatives of the energy with respect to the base-pair step parameters, however, is not straightforward as the restraint energy (eq 2) is a function of long-range intramolecular distances. We make use of analytical expressions for the derivatives developed by Gō and co-workers^{18,19} to treat the normal mode dynamics of a system of two molecules, each of which moves in dihedral angle space. The set of rigid body parameters used here to relate neighboring base-pair planes is identical in form to the variables previously used to describe the relative global positions and orientations of different molecules. The second derivative of the energy function and the molecular configuration at the energy minimum are used as input for normal-mode analysis.

Global Reference System. Each base pair of the energy-minimized DNA circle has a fixed coordinate frame defined in accordance with established guidelines.²⁰ The sequence of vectors connecting the origins of base-pair coordinate frames forms an approximately circular pathway in the minimum energy state. The step parameters used as independent variables in the normal-mode calculations, while useful for analyzing structural changes of DNA at the base-pair level, are less convenient for describing the global structural changes of a closed, circular DNA. We thus introduce a second coordinate frame on each base pair with one axis \mathbf{n}° directed from the origin toward the center of the circle, a second axis \mathbf{b}° oriented perpendicular to the plane of the circle, and the third axis \mathbf{t}° chosen to form a right-handed coordinate system ($\mathbf{t}^\circ = \mathbf{n}^\circ \times \mathbf{b}^\circ$). These three axes constitute a right-handed Frenet–Serret triad ($\mathbf{n}^\circ, \mathbf{b}^\circ, \mathbf{t}^\circ$), with elements corresponding respectively to the principal normal, binormal, and unit tangent vector at points on the DNA circle. For further analysis, we define a fourth axis ($\mathbf{O}_{BP} - \mathbf{P}$) $\times \mathbf{t}^\circ$, where \mathbf{O}_{BP} is the origin of the base-pair coordinate frame at a given hydrogen-bonded nucleotide unit in an arbitrary DNA structure, and \mathbf{P} is a point on the base-pair plane. This axis is useful for analyzing torsional motions, where a given point on each base-pair plane rotates around \mathbf{t}° . By analyzing the fluctuations of the molecule with respect to these axes, we obtain an image of overall global motion for each normal mode that complements the picture of local structural deformations provided by the base-pair step parameters.

Analytical Treatment. Given the linear differential equations which appear in the analytical theory of the normal modes of circular rings formed from naturally straight, inextensible, symmetric, elastic rods,^{14,15} the distortions from the circular configuration (the solutions of these equations) can be written as a linear combination of terms, each of which is proportional to the time-dependent function $e^{\pm i\omega t}$, where ω is the frequency. Furthermore, the fact that the axial curve is closed requires that the solutions be periodic, so that their dependence on arc length s (along the axial curve)

is similarly determined. That is, each of the terms in the linear combination must also be proportional to $e^{\pm i n \kappa^o s}$, where κ^o is the curvature of the circle and $n = 0, 1, 2, \dots$ (The wavelength λ_n of a normal mode is simply related to the integer n by the equation $\lambda_n = 2\pi/n\kappa^o$.) Introduction of these substitutions leads to a system of homogeneous linear equations with unknown constant amplitudes. The determinant made up of the coefficients of these amplitudes is a function of Ω , κ^o , ΔTw^o , n , and ω^2 , where ΔTw^o is the excess twist (of the circular equilibrium structure as a whole) and $\Omega = C/A$ is the ratio of the global twisting modulus to the global bending modulus. The determinant takes the form of a polynomial cubic in ω^2 , $M_3\omega^6 + M_2\omega^4 + M_1\omega^2 + M_0$, with the coefficients M_3 , M_2 , M_1 , and M_0 given by

$$M_3 = 2(\kappa^o)^{-10}(1 + (\kappa^o)^2 + n^6(\kappa^o)^4 - 2n^4(\kappa^o)^2((\kappa^o)^2 - 1) + n^2((\kappa^o)^4 - (\kappa^o)^2 + 1))$$

$$M_2 = -n^2(\kappa^o)^{-8} \left(\begin{aligned} &n^6(\kappa^o)^4(\Omega + 4) + 2n^4(\kappa^o)^2(\Omega + 2 - 5(\kappa^o)^2) \\ &+ n^2(4(\kappa^o)^2(2(\kappa^o)^2 - 1) + \Omega(1 + (\kappa^o)^2 - 3(\kappa^o)^4)) \\ &+ 2(\kappa^o)^4(\Omega - 1) + \Omega(3(\kappa^o)^2 + 1) \end{aligned} \right)$$

$$M_1 = n^4(n^2 - 1)(\kappa^o)^{-4} \left(\begin{aligned} &-(\Omega - 2)(\kappa^o)^2 + 2n^4(\Omega + 1)(\kappa^o)^2 \\ &-n^2(4(\kappa^o)^2 + \Omega((\kappa^o)^2 - 2)) \\ &-2\Omega^2(\kappa^o)^2(\Delta Tw^o)^2(n^2 - 1) \end{aligned} \right)$$

$$M_0 = -n^6(n^2 - 1)^2\Omega(n^2 - 1 - (\Delta Tw^o)^2\Omega^2) \quad (3)$$

The normal-mode frequency ω for given values of the four parameters Ω , κ^o , ΔTw^o , and n is obtained by setting the polynomial equal to zero and solving the cubic equation in (ω^2) , i.e., the roots of the polynomial determine the normal-mode frequencies of the elastic ring for that choice of parameters.

For each value of n , there are three distinct frequencies. The case n equal to 0 or 1 is special. For these values of n , both M_1 and M_0 , the only two of the four coefficients that depend on ΔTw^o , are zero. It follows that the six mode frequencies associated with these two values of n are independent of ΔTw^o . Of these six frequencies, five are zero, and the nonzero frequency is given by $(M_2/M_3)^{1/2}$. Finally, the circular symmetry inherent in the problem gives rise to a 2-fold degeneracy: in general there are two modes associated with each distinct normal-mode frequency.

For the case of the torsionally relaxed circle, where $\Delta Tw^o = 0$, the coefficients M_i in the dispersion relation are such that it is possible to give explicit expressions for the square of each of the three frequencies associated with a given n . The square of the frequency $\omega_{ip}^2(n)$ of the two degenerate in-plane modes for that n is

$$\omega_{ip}^2(n) = \frac{n^2(n^2 - 1)^2}{(R^o)^2((n^2 - 1)^2 + (R^o)^2(n^2 + 1))} \quad (4)$$

and the square of the two remaining frequencies, those of the out-of-plane modes, $\omega_{op}^2(n)$, are

$$\omega_{op}^2(n) = \frac{n^2(\Omega(n^2 + (R^o)^2 + 2) + 2(n^2 - 1))}{4(R^o)^2(n^2 + (R^o)^2)} \pm \frac{n^2\sqrt{(\Omega(n^2 + (R^o)^2 + 2) + 2(n^2 - 1))^2 - 8\Omega(n^2 - 1)(n^2 + (R^o)^2)}}{4(R^o)^2(n^2 + (R^o)^2)} \quad (5)$$

where $R^o (= 1/\kappa^o)$ is the radius of the circle. In these expressions R^o is measured in units of half the radius r of the elastic rod, about 5 Å in the case of DNA, and the frequency is measured in units of $(4/r^3)(A/\pi\rho)^{1/2}$. Here ρ is the density of the material from which the rod is made.

Results and Discussion

Minimum Energy Circular Configurations. We start the energy minimization from an open, perfectly straight DNA molecules with ideal B-DNA step parameters ($\theta_1 = \theta_2 = 0^\circ$, $\theta_3 = 36^\circ$, $\theta_4 = \theta_5 = 0$ Å, $\theta_6 = 3.4$ Å) at all dimeric units. The optimization balances two competing terms, i.e., the elastic energy in eq 1, which acts to preserve the B-DNA equilibrium geometry ($\theta_1'' = \theta_2'' = 0^\circ$, $\theta_3'' = 36^\circ$, $\theta_4'' = \theta_5'' = 0$ Å, $\theta_6'' = 3.4$ Å) of individual base-pair steps, and the end-to-end restraint energy in eq 2, which forces chain cyclization. The energy-minimization process is divided into two steps. Minimization is initially performed with restraints that force the overlap of the origins and normals (z -axes) of terminal base pairs and then is carried out with an additional restraint on the x -axes of the same residues. This two-step procedure guarantees successful ring closure and also ensures that the energy-minimized circular DNA configuration is torsionally relaxed, i.e., with the desired number of helical turns.

Using the energy-minimized structure as an initial conformation, we then create a series of slightly perturbed 200 base pair (bp) closed circular DNA molecules by changing the intrinsic Twist θ_3'' in eq 1, to study the effects of over- and undertwisting on the structure and dynamics of circular DNA. The uniform variation of θ_3'' mimics the known effects of temperature and added salt on DNA helical twisting.^{21–23} The potential energies found upon minimization are plotted versus the intrinsic Twist θ_3'' in Figure 1. A parabolic function of the form $y = a(x - x_0)^2 + y_0$, which fits the potential energy plot, is also depicted in the figure. The minimum energy value y_0 , the Twist angle x_0 at the minimum, and the coefficient a of the parabolic function are summarized in Table 1.

Mechanical Constants. The minimum energy state and curvature in Figure 1 can be used as follows to deduce mechanical constants that describe the global bending and twisting rigidity of an ideal, inextensible DNA elastic rod. Given that the potential energy of the rod arises from its overall bending and twisting, the minimum energy in the parabolic function in Figure 1 corresponds to the torsionally relaxed state of DNA, where the energy contribution comes purely from bending. Furthermore, the bending energy of an intrinsically straight rod closed into a circle is $2\pi^2 A/L$, where A is the bending rigidity and L is the length of the rod.²⁴ The bending rigidity is therefore easily calculated from the minimum energy values as $A = y_0(L/2\pi^2)$ and is also

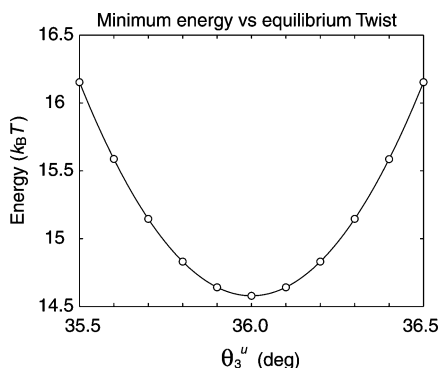


Figure 1. Minimized energy of a 200 bp closed circular DNA molecule, which is naturally straight in its equilibrium rest state and governed by an ideal elastic potential, plotted as a function of the intrinsic Twist, θ_3^u . The parabolic function, $y = a(x - x_0)^2 + y_0$, fitted to computed points of minimum energy (open circles), is depicted by a solid line. See Table 1 for numerical values of the fitted constants.

Table 1. Details of the Parabolic Function, $y = a(x - x_0)^2 + y_0$, Which Fits the Minimum Energy Plot in Figure 1, and Derived Mechanical Constants of a 200 bp DNA Circle, Which Is Naturally Straight in Its Equilibrium Rest State and Subject at the Level of Neighboring Base-Pair Steps to an Ideal Elastic Potential

| x_0 (deg) | y_0 ($k_B T$) | a ($k_B T/\text{deg}^2$) | bending rigidity ^a (10^{-19} erg-cm) | twisting rigidity ^a (10^{-19} erg-cm) |
|----------------|----------------------|---------------------------------|---|--|
| 36 | 14.579 | 6.298 | 2.066 (2.098) | 2.892 (2.879) |

^a Mechanical constants calculated on the basis of the normal-mode frequencies of the corresponding linear DNA chain are reported in parentheses.

reported in the table. Similarly, the curvature $2a$ of the parabolic function in Figure 1 is related to the twisting rigidity C by $a = Cn_B^2/2L$, where n_B is the number of base-pair steps. Cyclization of a linear DNA of n_B bp with intrinsic Twist $x = \theta_3^u$ introduces additional torsional stress, $-n_B(x - x_0)$, where x_0 is the equilibrium Twist of the torsionally relaxed molecule. The increase in twist raises the elastic energy by $Cn_B^2(x - x_0)^2/2L$,²⁴ corresponding to an increment of $a(x - x_0)^2$ in the computed energy (Figure 1). Therefore, the global twisting rigidity is easily calculated and also reported in Table 1. The values of the bending and twisting rigidities of a linear 200 bp DNA molecule with the same conformational features are included for comparison in the table. The latter constants, which are derived from the computed normal-mode bending and twisting frequencies of an open chain subject to the same dimeric potential,¹ are remarkably close to the values calculated from the minimum energy of the circular molecule.

It should be noted that the above expressions for A and C are only valid for the current simplified DNA force field, where the Twist in the minimum energy structure is nearly constant at every base-pair step. In the case of real DNA,⁸ the uptake of Twist in the minimum energy state is not uniform, with local variations associated with intrinsic bending, correlations between base-pair parameters, etc.^{25,26} The preceding calculation of mechanical constants does not hold in such instances.

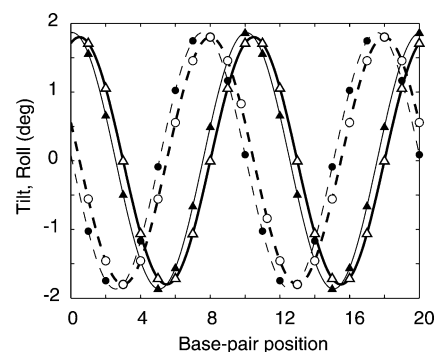


Figure 2. Sequential variation of Tilt° and Roll° angles (Δ and \circ symbols, respectively) along the contour of a 200 bp torsionally relaxed DNA circle which is naturally straight in its equilibrium rest state and subject to an ideal elastic potential. Cosine functions fitted to the data (see Table 2) are represented respectively by thick solid and dashed curves. Values of Tilt and Roll (filled-in Δ and \circ symbols) at the moment when the potential energy is raised by $k_B T/(2 \times 10^4)$ along the lowest frequency ($n = 0$) torsional mode are also plotted. Cosine functions fitted to the data are represented by thin solid and dashed curves, respectively. Because of the repetitive pattern of conformational variation, data are shown for only the first 20 steps of the chain.

Table 2. Base-Pair Step Parameters, in Degrees, at the m th Dimer Step of an Ideal, Inextensible^a Circular DNA Molecule of n_B Base Pairs and Intrinsic Twist θ_3^u in the Minimum Energy State

| n_B | θ_3^u | Tilt° | Roll° | Twist° |
|-------|--------------|---------------------------|--------------------------------|--------|
| 160 | 36 | $2.25 \cos(36(m - 0.50))$ | $2.25 \cos(36(m - 0.50) + 90)$ | 36 |
| 180 | 36 | $2.00 \cos(36(m - 0.50))$ | $2.00 \cos(36(m - 0.50) + 90)$ | 36 |
| 200 | 35.5 | $1.80 \cos(36(m - 0.74))$ | $1.80 \cos(36(m - 0.74) + 90)$ | 36 |
| 200 | 36 | $1.80 \cos(36(m - 0.50))$ | $1.80 \cos(36(m - 0.50) + 90)$ | 36 |
| 200 | 36.5 | $1.80 \cos(36(m - 0.12))$ | $1.80 \cos(36(m - 0.12) + 90)$ | 36 |
| 220 | 36 | $1.64 \cos(36(m - 0.50))$ | $1.64 \cos(36(m - 0.50) + 90)$ | 36 |
| 240 | 36 | $1.50 \cos(36(m - 0.50))$ | $1.50 \cos(36(m - 0.50) + 90)$ | 36 |

^a (Shift°, Slide°, Rise°) = (0 Å, 0 Å, 3.4 Å).

Smooth Bending. Figure 2 illustrates the uptake of bending along the contour of the 200 bp torsionally relaxed DNA circle in its minimum energy state. Because the same conformational pattern is repeated every 10 bp, step parameters in the minimum energy structure, which are henceforth termed Tilt°, Roll°, Twist°, ..., are reported for only a fragment of the chain, here the first 20 bp steps. [These “static” values should not be confused with the “dynamic” fluctuations of step parameters which are reported in later sections.] As expected from the theory,²⁴ the values of Twist° are constant (36°) in the minimum energy state and therefore not shown. The sinusoidal changes in Tilt° and Roll° follow the characteristic pattern of “smooth” DNA bending,^{27–29} with one parameter attaining a maximum or minimum value when the other is zero. Details of the best-fit cosine functions, which are plotted in the figure, are summarized in Table 2. As is clear from the expressions, the sequential changes of Tilt° and Roll° differ in phase by 90°. The curves that fit Tilt° and Roll° values in DNA with different values of intrinsic Twist, θ_3^u , are also summarized in the table. The

latter curves, reported for chains of 200 bp, are also related to each other by a 90° phase shift.

In a later section, we study the dependence of normal-mode frequencies on the length of DNA. For this reason, we have constructed torsionally relaxed DNA circles of different chain lengths (160, 180, 220, 240 bp) using the same ideal force field. The values of Tilt° and Roll° in the minimum energy state are again well approximated by single cosine curves, which are summarized in Table 2. Step parameters, in degrees, at the m th dimer steps of the minimum energy structures fit the following general form if n_B , the number of base pairs, is a multiple of 10:

$$\begin{aligned}\text{Tilt}^\circ &= \left(\frac{360}{n_B}\right)\cos(36(m - 0.5)) \\ \text{Roll}^\circ &= \left(\frac{360}{n_B}\right)\cos(36(m - 0.5) + 90) \\ \text{Twist}^\circ &= 36\end{aligned}\quad (6)$$

The inverse dependence in this expression of the amplitudes of Tilt° and Roll° on n_B means that the curvature of the molecule is proportional to the amplitude of local conformational changes. Since curvature is the inverse of the radius of a circle and the radius of a circular DNA molecule is proportional to the number of base pairs, curvature is also proportional to the inverse of n_B . Thus, when the amplitude of Tilt° and Roll° variations is larger, curvature is larger, and when the amplitude is smaller, curvature is smaller.

If, as considered here, the elastic constants f_{ii} impeding Tilt and Roll deformations are identical, the circular state remains a conformational energy minimum even if the constant -0.5 in eq 6 is replaced by other values. The restraint energy of such a molecule, however, differs from the ideal closed molecule in being greater than, albeit very close to, zero. Thus, the constant in the phase of the cosine functions in eq 6 is affected by the restraints in eq 2. For example, if we place restraints on the y -axes, rather than the x -axes, of terminal base pairs, the constant is -3 . The effect of the starting structures on the optimized circular state, however, is limited.

Uniform Twisting and Uptake of Energy. Figure 3 shows the contributions of Tilt, Roll, and Twist to the dimer step energy at sequential positions along three 200 bp DNA circles in different minimum energy configurations: a torsionally relaxed molecule, an overtwisted chain, and an undertwisted chain with respective intrinsic Twist angles, θ_3^u , of 36°, 35.5°, and 36.5°. Because the energetic patterns repeat every 10 bp, data are plotted, as above, for only the first 20 bp steps. As reported in Table 2, the value of Twist° in the minimum energy configuration shows only limited dependence on the assumed intrinsic Twist. As a result, when the intrinsic Twist angle is decreased, Twist° exceeds the intrinsic value and the DNA is overtwisted. In the same way, when the intrinsic value of Twist is increased, the DNA becomes undertwisted. The change of intrinsic Twist θ_3^u from the value of 36° in the torsionally relaxed state introduces a constant contribution to the dimer energy at every base-pair

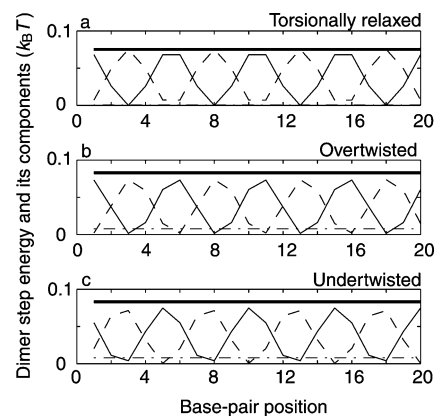


Figure 3. Dimer step energy (thick solid lines) and its bending and twisting components (Tilt: thin solid lines; Roll: dashed lines; Twist: dash-dotted lines) of (a) torsionally relaxed, (b) overtwisted, and (c) undertwisted DNA molecules, which are naturally straight at equilibrium, subject to an ideal elastic potential, and closed via energy minimization into 200 bp circles. The intrinsic Twist, θ_3^u , is fixed respectively at 36°, 35.5°, and 36.5° in the three structures. Because of the regular energetic patterns, data are shown for only the first 20 steps.

step, a well-known property of a naturally straight, homogeneous elastic rod.²⁴ Moreover, the energetic contributions associated with the deformations of Tilt and Roll are compensatory so that the dimer step energy is nearly constant along the chain contour. The uniform energy density along the chain is another well-known property of a naturally straight elastic rod with constant curvature.²⁴ This uniformity does not hold, however, if the chain is subject to local anisotropic bending, i.e., different force constants f_{ii} for Tilt and Roll.

Motions of Relaxed DNA Circles. The normal-mode analysis of energy-minimized DNA circles provides information on the frequencies and collective motions of the closed chain. We concentrate here on the very low frequency normal modes responsible for large-scale deformations of structure, studying both torsionally relaxed DNA and molecules with torsional stress. The normal modes of lowest frequency show one of three types of large-scale deformation, namely in-plane, out-of-plane, and torsional motions. These motions, which are consistent with the predictions of elastic rod theory,^{14,15} are illustrated schematically in Figure 4 and reported as a function of frequency in the color-coded “spectrum” in Figure 5(a). The in-plane bending motion of the torsionally relaxed molecule involves changes in Tilt and Roll, whereas the out-of-plane bending motions always involve torsion. Local bending deformations also accompany the global torsional motions.

“Free” Torsional Motions. The DNA remains circular in the lowest (nearly zero) frequency mode, with the molecule rotating as a whole about its helical axis; see Figures 4(a) and 5(a), and the Supporting Information. Such behavior is predicted by the theory of elastic rod deformations, i.e., modes associated with n equal to 0 or 1 must be nonflexural and the rotation of the DNA in the $n = 0$ torsional mode is unimpeded.³⁰

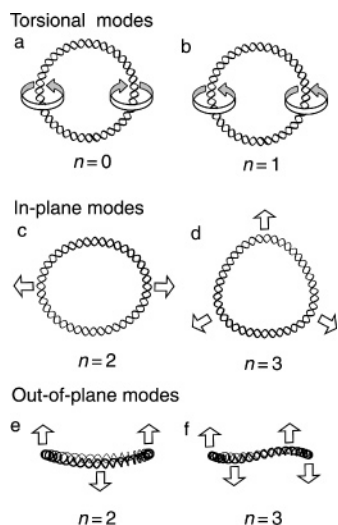


Figure 4. Schematic illustration of selected low-frequency normal modes of a closed circular double helical DNA molecule. The arrows denote the directions of bending or twisting in each mode. Images (a,c,e) depict the lowest frequency mode in each of the three types of global motions and images (b,d,f) the second lowest frequency modes. The values of n refer to indices used in elastic rod theory^{14,15} to differentiate modes within the same class of motions. Double helical images generated with MolScript.³³

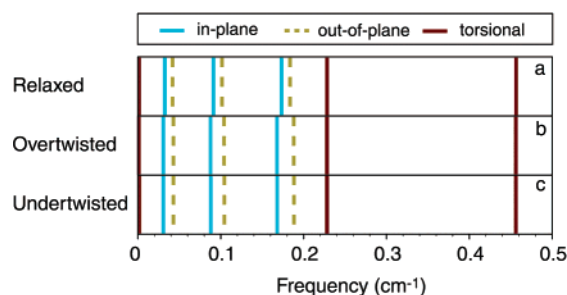


Figure 5. Color-coded spectra of the lowest frequency torsional (unbroken red line), in-plane (unbroken blue line), and out-of-plane (broken green line) modes of a 200 bp DNA molecule, which is naturally straight in its equilibrium rest state, subject to an ideal elastic potential, and closed into a circle with different values of intrinsic Twist: (top) torsionally relaxed ($\theta_3^u = 36^\circ$); (middle) overtwisted ($\theta_3^u = 35.5^\circ$); (bottom) undertwisted ($\theta_3^u = 36.5^\circ$).

The sequential variation of base-pair step parameters which accompanies the “free” torsional motion is compared in Figure 2 with the corresponding values in the equilibrium reference state (filled-in vs corresponding open symbols). The plot captures the values of Roll and Tilt in a 20 bp fragment of the 200 bp circle at the instant when the energy of the DNA is raised by $k_B T / (2 \times 10^4)$. The very low-energy threshold is a consequence of the extremely low frequency, i.e., small energy change, of the mode and the limitation of normal-mode analysis to conformational fluctuations in the vicinity of the minimum energy state. (Step parameters lie far away from the reference state if the mode is assigned a higher energy.) Twist, by contrast, remains constant during the process. Thus, the nearly free rotation of the helix as a whole arises from concerted changes in local bending, rather

than twisting, over a 10 bp helical repeat. The regular pattern of Roll and Tilt variations is emphasized by the cosine functions superimposed on the computed points in Figure 2.

As long as the variation in bending parameters is small compared to the range of Roll $^\circ$ and Tilt $^\circ$ in the minimum energy state (the conditions under which normal-mode analysis holds), the Roll and Tilt values will simply move back and forth along the chain contour, i.e., abscissa in Figure 2, as the amplitude and direction of fluctuations change over time. The resulting shift in the sites of maximum and minimum bending leads to the global rotational motion. For example, the minima of Roll $^\circ$ (thick solid lines) in Figure 2 occur at positions where the minor groove edges of base pairs 3, 13, 23, etc. face the center of the circle. The shift of phase associated with the normal mode moves base-pair steps such as these on the inside of the circle to the outer surface of the molecule, and vice versa, thereby producing rotational motion around the helical axis.

In-Plane Bending. The second and third lowest frequency modes correspond to in-plane motions, which deform the DNA circle to elliptical shapes; see Figure 4(c) and the Supporting Information. These modes with nearly equivalent frequencies differ only in the direction of global distortion, one mode generating a family of ellipses with major and minor axes rotated $\sim 45^\circ$ with respect to the corresponding axes of the second family of structures. Both the pure in-plane character of the modes and the equivalence of the frequencies are consistent with theoretical predictions. The directional differences in the in-plane bending modes are seen in the fluctuations of base-pair origins in the nonequilibrium states with respect to the (\mathbf{n}° , \mathbf{b}° , \mathbf{t}°) Serret-Frenet frames embedded in each base pair of the minimum energy (perfectly circular) reference state. The plots in Figure 6-(a,b) show the base-pair displacements at the moment when the potential energy of the DNA in the two modes is raised by $k_B T / 2$. The uniformly zero displacements along the \mathbf{b}° axes of the planar circle (dashed lines in the figure) confirm the pure, in-plane nature of molecular deformation, and the larger sinusoidal displacements along the \mathbf{n}° and \mathbf{t}° axes (solid curves) the elliptical shapes. The major axes of the ellipses captured in Figure 6(a,b) run parallel to the vectors that join base pairs (20, 120) and (95, 195), respectively. These pairs of points correspond to the minima in the \mathbf{n}° -axis displacements in the two plots. The 25 bp phase shift of corresponding curves of the two in-plane modes accounts for the different directions of global motion. The similar, yet out-of-phase pattern of conformational change observed here is reminiscent of the doubly degenerate pure bending modes of a linear DNA, with overall chain deflections in perpendicular directions.¹ Like the open chain, the closed DNA effects global distortions exclusively through Tilt and Roll, thereby qualifying as a bending mode; see Figure 7(a, b). As with the linear molecule, the degeneracy of the in-plane modes of a circular molecule is expected to break down for particular sequential repeats.

Examination of Figure 7(a,b) shows that the maximum or minimum fluctuations of Tilt and Roll appear at positions where Tilt $^\circ$ and Roll $^\circ$ assume a maximum or minimum in the equilibrium state and that the fluctuations are zero at

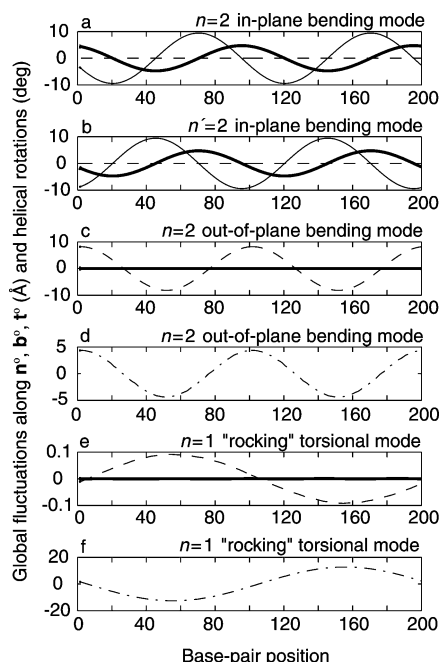


Figure 6. Displacement of base-pair origins and rotation of base-pair axes at the moment when the potential energy is raised by $k_B T/2$ in selected normal modes of a 200 bp torsionally relaxed DNA circle which is naturally straight in its equilibrium rest state. Displacements (thin solid, dashed, and thick solid lines) measured respectively along the n° , b° , t° axes of Serret-Frenet frames embedded in each base pair of the minimum energy DNA circle and found in (a,b) the pair of lowest frequency ($n = 2$) in-plane bending modes; (c) one of the lowest frequency ($n = 2$) out-of-plane bending modes; (e) one of the second lowest ($n = 1$) frequency “rocking” torsional modes. Rotational fluctuations (dash–dotted line) found in (d) one of the lowest frequency ($n = 2$) out-of-plane bending modes and (f) one of the second lowest ($n = 1$) frequency “rocking” torsional modes.

steps where equilibrium values are zero. That is, the points of maximum or minimum Tilt and Roll do not change position in these two modes, a further indication that the bending motions are restricted to the plane of the energy-optimized circular structure. This pattern of dimer deformation in each of the modes is quite distinct from the traveling waves of local bending associated with the “free” torsional mode. The in-plane bending modes differ in phase such that the largest changes in curvature in one mode occur at positions where there are no deformations in the other mode and vice versa.

Addition of the two in-plane bending modes, as represented in Figure 7(a,b), creates a standing wave of chain deformation similar in character to each of its degenerate components, i.e., the closed molecule oscillates between circular and elliptical shapes via localized compensatory changes in Tilt and Roll. If the two modes are not in phase, the linear combination of modes produces a traveling elliptical wave with the sites of maximal conformational distortion moving over time along the chain contour (see the Supporting Information). The direction of motion and the magnitude of elliptical distortion of the traveling wave depend on the difference in phase angle $\Delta\delta$, i.e., the direction

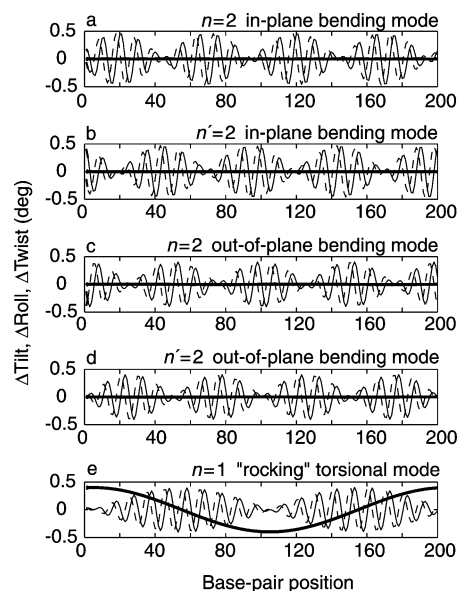


Figure 7. Fluctuations of local angular “step” parameters which are collectively responsible for selected normal modes of a 200 bp torsionally relaxed DNA circle which is naturally straight in its equilibrium rest state and subject to an ideal elastic potential: (a,b) the pair of lowest frequency ($n = 2$) in-plane bending modes; (c,d) the pair of lowest frequency ($n = 2$) out-of-plane bending modes; (e) one of the pair of second lowest frequency ($n = 1$) torsional modes. Plots illustrate the fluctuations of Tilt (thin solid lines), Roll (dashed lines), and Twist (thick solid lines) along the contour of the DNA molecule at the moment when the potential energy of the molecule is raised by $k_B T/2$; fluctuations are reversed a half cycle later of the mode.

of the movement reverses if the sign of $\Delta\delta$ (defined over the range $-180^\circ < \Delta\delta \leq 180^\circ$) is changed. The proportions of the traveling ellipse are constant only when $\Delta\delta = \pm 90^\circ$. Otherwise, both the proportions and the sites of elliptical deformation vary with time.

The local step parameters responsible for the one of the in-plane bending modes, obtained by adding the computed (ΔTilt , ΔRoll) deformations to the (Tilt° , Roll°) values that describe the minimum energy state, are presented in Figure 8. The agreement in phase of the (ΔTilt , ΔRoll) variation with the trigonometric equations (Table 2) that define the (Tilt° , Roll°) minimum energy state works positively at some positions, increasing the amplitude, and negatively at others, decreasing the amplitude. The amplitude assumes a maximum at the 20th and 120th base-pair steps, and minima at the 70th and 170th base-pair steps in the plot. As noted above, the magnitude of the amplitude is proportional to the curvature. Therefore, at the former pair of antipodal base-pair steps, the curvature is larger, and at the latter steps, the curvature is smaller than in the minimum energy structure. A half cycle later, the situation reverses, with lesser curvature found at the former positions and greater curvature at the latter ones.

Out-of-Plane Bending. The fourth and fifth lowest normal modes, also of close frequency, describe out-of-plane, cup-like bending deformations of the DNA circle; see Figure 4(e) and the Supporting Information. The null displacement, in

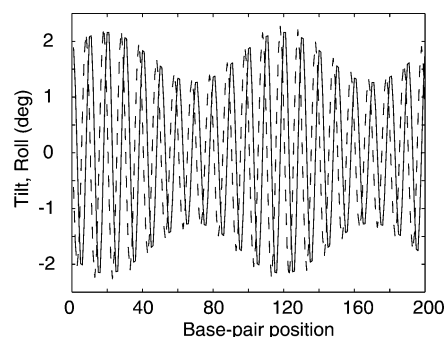


Figure 8. Values of Tilt and Roll (solid and dashed lines) along the contour of a 200 bp torsionally relaxed DNA circle at the moment when the potential energy is raised by $k_B T/2$ by lowest frequency ($n = 2$) in-plane bending motions. Data are obtained by adding the bending fluctuations in Figure 7(a) to the energy-optimized parameters of the covalently closed, molecule in Figure 2.

Figure 6(c), of base-pair origins in directions other than \mathbf{b}° points to the pure out-of-plane character of the motions and the uptake of deformation through Tilt and Roll in Figure 7(c) to the role of bending. The major difference between the two out-of-plane modes is the direction of distortion, expressed at the local level by a 25 bp shift in the pattern of conformational fluctuations and at the global level by an orientational change of $\sim 45^\circ$. Notably, the profiles of conformational change responsible for the out-of-plane modes are closely related to those associated with the in-plane deformations; see Figure 7(a–d). Values of ΔTilt and ΔRoll associated with in-plane deformations attain local maxima or minima at the base-pair steps that are unchanged during out-of-plane distortions and vice versa.

There is a rotational motion of the bases in the out-of-plane modes similar to that found in the lowest frequency torsional mode, the “free” torsional mode. The degree of rotation varies along the chain contour, and the direction of rotation is of the opposite sense at positions 50 bp apart. If adjacent segments of a perfect circular rod were to rotate in the opposite sense, torsional stress would build up between them, but as seen in Figure 7(c,d), ΔTwist is approximately zero in the out-of-plane modes. The torsional stress is relieved by the displacement of antipodal segments of the chain perpendicular to the plane of the circle. The fluctuations of the base-pair origin along the \mathbf{b}° axis in Figure 6(c) are in perfect phase with the rotation of bases, monitored in Figure 6(d) by the positions of $(\mathbf{O}_{\text{BP}} - \mathbf{P})$ vectors on successive base pairs. Such deformations also agree with the theoretical expectation that the out-of-plane modes entail torsional motions.

Higher-Frequency Modes. The majority of very low frequency modes of the ideal DNA chain are either in- or out-of-plane bending motions (see the color-coded spectrum of frequencies in Figure 5(a)). Furthermore, the two types of modes occur as closely spaced pairs, with the 2-fold degeneracy of each mode leading to four independent motions of close frequency. The pure in-plane or out-of-plane character of the motions, however, disappears as the frequencies become larger. For example, the out-of-plane fluctuations (along the \mathbf{b}° -axis) of the in-plane modes become

increasingly larger, and it becomes impossible to tell whether the mode should be classified as an in-plane or an out-of-plane mode. That is, fluctuations along \mathbf{b}° become comparable to those along \mathbf{n}° and \mathbf{t}° .

Like the bending modes of a naturally straight linear DNA molecule, the number of pure in-plane or pure out-of-plane bending modes of the circular chain is limited in number. For both in- and out-of-plane modes, ΔTilt and ΔRoll fluctuate in cycles of 10 bp steps, with null fluctuations of parameters occurring simultaneously at several steps (nodes). Reexamination of Figure 7(a–d) reveals four such nodes, separated by 50 bp increments, for the lowest frequency in-plane and out-of-plane bending modes of a 200 bp closed circle. The number of nodes increases, and the distance between adjacent nodes decreases as the frequency becomes higher. If adjacent nodes approach too closely, ΔTilt and ΔRoll can no longer fluctuate in cycles of 10 bp steps, thereby limiting the number of pure in-plane or out-of-plane modes. The 200 bp DNA circle has only eight pairs of fairly pure in-plane modes and eight pairs of fairly pure out-of-plane modes, with the highest frequencies of the in-plane modes being 0.869 cm^{-1} and 0.870 cm^{-1} , and those of the out-of-plane modes 0.877 cm^{-1} and 0.878 cm^{-1} . There are 18 nodes in these four higher frequency modes.

A second ($n = 1$) torsional mode, which preserves the circular structure of DNA and allows for the opposing rotation of base pairs around the helical axis, is found at higher frequency (Figures 4(b) and 5(a) and the Supporting Information). As is clear from Figure 6(e,f), the rotational motion (illustrated in the latter plot) is accompanied by small ($\pm 0.1\text{ \AA}$) out-of-plane base-pair displacements (dashed curves in the other plot). The latter features are consistent with the small oscillatory rocking motion predicted by elastic rod theory for this mode.¹⁴ [The term rocking is characteristic of a standing mode; the motions of the traveling modes generated by the linear combination of degenerate $n = 1$ torsional modes resemble those of a precessing top.] The opposing rotations at antipodal sites on the circle introduce torsional stress on the intermediate regions, leading to the build-up of ΔTwist illustrated by heavy solid lines in Figure 7(e). The bending angles are unchanged at the sites of maximum over- and underwinding but are maximally perturbed when ΔTwist is zero. The patterns of ΔTilt and ΔRoll resemble those for the out-of-plane bending motions in terms of the $\sim 10\text{ bp}$ phase of the computed fluctuations. The sites that bend more strongly or become more straightened around the closed structure are more widely spaced along the chain contour than the sites of strongest and weakest bending in the out-of-plane mode, i.e., repetition at $\sim 100\text{ bp}$ vs $\sim 50\text{ bp}$ intervals. A degenerate torsional mode of the same type introduces torsional stress and bends the DNA in the same fashion but is displaced 50 bp further along the chain contour. The degeneracy of the $n = 1$ torsional mode also matches theoretical expectations.

Motions of Supercoiled Molecules. *Normal-Mode Frequencies.* Slight over- or undertwisting of the DNA circle introduces subtle changes in the computed normal-mode frequencies. As evident from the color-coded spectra of lowest frequency modes in Figure 5(a–c), the torsional

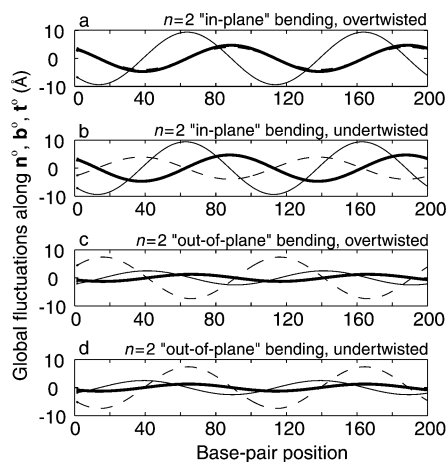


Figure 9. Displacement of base-pair origins of (a,c) overtwisted ($\theta_3^u = 35.5^\circ$) and (b,d) undertwisted ($\theta_3^u = 36.5^\circ$) DNA circles along the \mathbf{n}° , \mathbf{b}° , \mathbf{t}° axes of Serret-Frenet frames embedded in each base pair of the minimum energy DNA circle. Data reported at the moment when the potential energy of the naturally straight, 200 bp molecule is raised by $k_B T/2$ in selected normal modes: (a,b) one of the lowest ($n = 2$) frequency, predominantly in-plane bending modes; (c,d) one of the lowest ($n = 2$) frequency, predominantly out-of-plane bending modes. See legend to Figure 6.

modes (unbroken red lines) of the overtwisted ($\theta_3^u = 35.5^\circ$) and undertwisted ($\theta_3^u = 36.5^\circ$) molecules appear to coincide with those of the torsionally relaxed circle of the same length (200 bp), but the spacing between in-plane and out-of-plane frequencies (unbroken blue and broken green lines, respectively) differs. The in-plane bending motions of the supercoiled chains are consistently lower in frequency (energy) and the out-of-plane motions are consistently higher in value than the corresponding modes of the relaxed circle, with the differences becoming more pronounced as the frequencies of the modes increase. These trends match theoretical expectations as detailed below.

Mixed Bending Modes. Elastic rod theory predicts that pure in-plane or out-of-plane modes do not exist when the ideal rod is torsionally stressed. This is also true in our DNA model. Figure 9 illustrates the mixed nature of global structural fluctuations for two 200 bp chains with intrinsic Twist 35.5° and 36.5° . As is clear from Figure 9(a,b), the base-pair origins undergo small (± 3 Å) out-of-plane displacements along the \mathbf{b}° axes of the planar circle (dashed curves) as the molecule concomitantly deforms to elliptical shapes, and as evident from Figure 9(c,d), the chain fluctuates along the \mathbf{n}° and \mathbf{t}° axes in the plane of the ring (solid curves) as it also bends out-of-plane to cup-like shapes. Thus, the former mode is no longer a pure in-plane bending mode, and the latter is no longer a pure out-of-plane bending mode if the circular molecule is torsionally stressed.

Comparison of Figure 9 with the corresponding plots in Figure 6(a–c) for the torsionally relaxed circle shows that the normal modes of the supercoiled rings are combinations of pure in-plane and pure out-of-plane bending modes. For example, the low-frequency bending mode of the overtwisted DNA molecule in Figure 9(a), with intrinsic Twist 35.5° , is obtained by combining the in-plane mode of the relaxed

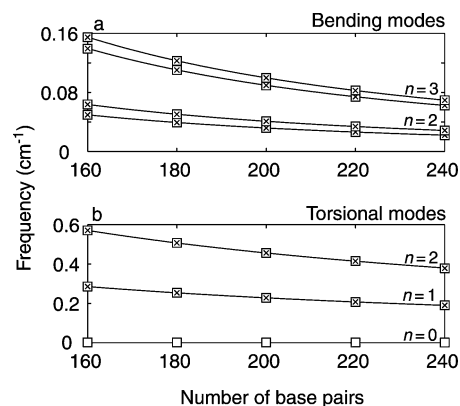


Figure 10. Normal-mode frequencies of (a) the two lowest ($n = 2, 3$) pairs of in-plane bending modes and the two lowest ($n = 2, 3$) pairs of out-of-plane bending modes and (b) the three lowest ($n = 0, 1, 2$) torsional modes, as a function of chain length, of a torsionally relaxed circular DNA, which is naturally straight in its equilibrium rest state and subject to an ideal elastic potential. The degeneracy of certain modes is evident from the computed frequencies, which are distinguished by the open boxes and cross symbols. The theoretically predicted chain length dependence of the frequencies, based on elastic rod theory,^{14,15} is shown as solid lines. Note that the out-of-plane modes have higher frequencies than the in-plane modes of corresponding n .

circle from Figure 6(a), with the out-of-plane mode in Figure 6(c). Figure 9(b–d) are obtained in a similar fashion.

The variation of Tilt and Roll reflects this combination of pure in-plane and out-of-plane bending motions. The fluctuations of Δ Tilt and Δ Roll in the lowest frequency bending modes of the over- and undertwisted DNA circles are a mixture of the change in step parameters that accompany pure in-plane and out-of-plane bending of the relaxed circle. The labels of the mixed bending modes are described by the more dominant of the two modes. Thus, the “in-plane” modes of the supercoiled circles have more pure in-plane than pure out-of-plane character, and the pure out-of-plane deformations outweigh the pure in-plane contributions to Δ Tilt and Δ Roll in the out-of-plane modes.

Comparison with Theory. Chain Length Dependence. To study the dependence of the normal modes on chain length, we created five torsionally relaxed circular DNAs of different length—160, 180, 200, 220, 240 bp, and performed normal-mode analyses of each chain. Figure 10(a) shows the frequencies of the two lowest pairs of in-plane bending modes and the two lowest pairs of out-of-plane bending modes as a function of chain length. The degeneracy of the bending modes is evident from the superposition of computed frequencies, with one of each pair of modes denoted by an open box and the other by a cross symbol. The overlap of these values with the theoretically predicted frequencies^{14,15} of an inextensible, naturally straight, homogeneous rod closed into a circle, shown by the solid curves in the figure, is remarkable (the numerical agreement is within 3×10^{-4} cm⁻¹).

As mentioned earlier, the theoretical frequencies are determined in units of $(4/r^3)(A/\pi\rho)^{1/2}$, where r is the radius of the elastic rod and ρ is its mass density. To make the comparison with the calculated values, we use a bending

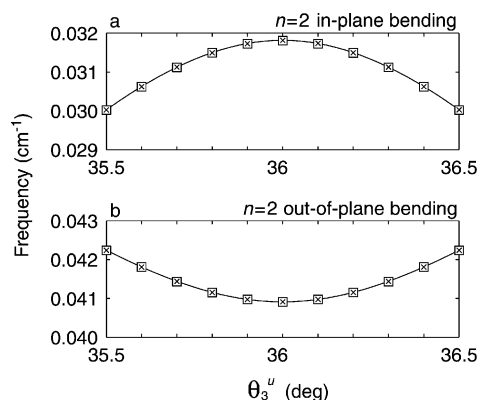


Figure 11. Normal-mode frequencies of the lowest ($n = 2$) pair of (a) in-plane and (b) out-of-plane bending modes, as a function of intrinsic Twist, θ_3^u , of a 200 bp circular DNA molecule, which is naturally straight in its equilibrium rest state. See legend to Figure 10.

rigidity A of 2.066×10^{-19} erg-cm deduced in Table 1 from the minimum energy circular state and set the radius r to 9.45 Å. This value of r is obtained by equating the inertial moment around the longitudinal axis of a straight rod of circular cross-section ($M r^2$) to the corresponding value for a B-DNA helix (calculated as a summation over all atoms of the DNA, $\sum m_i r_i^2$, where m_i is the mass of i th atom and r_i is the displacement of the atom from the helical axis). See ref 31 for the computational procedure used to locate the helical axis. A mass density of DNA of 0.065 g/mol-Å³ is used. Finally, the circular frequency unit (1.17×10^{12} Hz) has been converted to wavenumbers, cm^{-1} .

The number n in Figure 10 is the index used in the theory to differentiate normal modes within the same class of motions (i.e., in-plane, out-of-plane, or torsional modes) and is equal to half the number of nodes found in the mode. As evident from the figure and from earlier discussion of the torsionally relaxed 200 bp circle, out-of-plane modes have higher frequencies than in-plane modes of corresponding n . The similar chain length dependence of the computed and theoretically predicted frequencies of the three lowest torsional modes is apparent in Figure 10(b). The agreement between numerical values is again quite good, despite the fact that the theoretically predicted frequency of the $n = 0$ torsional mode is zero and the computed values are small nonzero values.

Twist Dependence. As noted above, the DNA circle can be supercoiled by changing the value of the intrinsic Twist θ_3^u . For example, a change of the intrinsic Twist of a 200 bp DNA circle from the value of 36° found in the torsionally relaxed state to 35.5° introduces excess Twist in the molecule, $200 \times (36 - 35.5)^\circ = 100^\circ$. The latter value is one of the variables used in the analytical treatment of the normal-mode frequencies of a closed elastic ring.^{14,15} The theoretically predicted frequencies of the lowest ($n = 2$) in-plane and out-of-plane bending modes are compared with values computed, respectively, for over- and undertwisted 200 bp circular DNA molecules in Figure 11(a,b). The agreement is again quite good, with the frequencies of the dominant in-plane mode reduced when the molecule is over- or

undertwisted and the frequencies of the dominant out-of-plane mode increased under the same conditions.

In agreement with the theoretical method described in connection with eq 3 to determine the normal-mode frequencies, the torsional mode frequencies are nearly independent of excess twist. The respective frequencies of the $n = 1$ and $n = 2$ torsional modes of a 200 bp circle are predicted by the theory to be 0.2281 and 0.4561 cm^{-1} . The average values of the corresponding normal-mode frequencies of 11 different DNA circles, with intrinsic Twist varied from 35.5° to 36.5° at increments of 0.1° , are 0.2282 and 0.4562 cm^{-1} . Each of these modes is doubly degenerate, with some slight differences in the computed standard deviations of normal-mode frequencies: 2.82 vs $2.25 \times 10^{-6} \text{ cm}^{-1}$ and 4.60 vs $2.96 \times 10^{-6} \text{ cm}^{-1}$ for the respective modes. The very small deviations show that the computed frequencies are essentially independent of added Twist, in further agreement with predictions of elastic rod theory.

Conclusions

The motions of an ideal, closed circular DNA molecule obtained in the present normal-mode calculations show remarkable agreement with the theoretically predicted dynamic properties of an elastic rod. The energy-optimized closed circular states and the types of low frequency motions of a 200 bp molecule which is naturally straight in its relaxed linear state, inextensible, and capable of isotropic bending and twisting of adjacent base pairs, reproduce a wide variety of features, including (1) the uniformity of twist density and energy density in the minimum energy state; (2) the near zero frequency “free” torsional mode of the torsionally relaxed circle; (3) the higher-order torsional rocking modes and the pure in-plane and out-of-plane bending motions of the relaxed circle; (4) the mixed bending modes of the supercoiled chain; (5) the degeneracy of modes; and (6) the changes in normal-mode frequencies with variation of chain length and imposed supercoiling. The successful comparison validates extension of the computational procedure to study effects of specific base sequences on the supercoiled states and global motions of more realistically modeled DNA minicircles.

The curves fitted to the sequential variation of step parameters in both the minimum energy configuration and the different normal modes reveal the interplay between local conformational motions and global chain dynamics. The patterns of local conformational deformation responsible for the overall motions of the closed duplex persist in more realistically modeled DNA minicircles and, as illustrated in the companion article,³² can be used to understand the effects of intrinsic curvature on large-scale global motions.

Acknowledgment. Support of this work through U.S.P.H.S. Grant GM34809 and the New Jersey Commission on Science and Technology (Center for Biomolecular Applications of Nanoscale Structures) is gratefully acknowledged. Computations were carried out at the Rutgers University Center for Computational Chemistry.

Supporting Information Available: Animation files of the normal modes of a 200 bp, torsionally relaxed, closed circular DNA molecule, which is naturally straight in its equilibrium rest state and subject to an ideal elastic potential. This material is available free of charge via the Internet at <http://pubs.acs.org>.

References

- (1) Matsumoto, A.; Olson, W. K. Sequence-dependent motions of DNA: a normal mode analysis at the base-pair level. *Biophys. J.* **2002**, *83*, 22–41.
- (2) Gō, N.; Noguti, T.; Nishikawa, T. Dynamics of a small protein in terms of low-frequency vibrational modes. *Proc. Natl. Acad. Sci., U.S.A.* **1983**, *80*, 3693–3700.
- (3) Levitt, M.; Sander, C.; Stern, P. S. Protein normal-mode dynamics: trypsin inhibitor, crambin, ribonuclease and lysozyme. *J. Mol. Biol.* **1985**, *181*, 423–447.
- (4) Nishikawa, T.; Gō, N. Normal modes of vibration in bovine pancreatic trypsin inhibitor and its mechanical property. *Proteins* **1987**, *2*, 308–329.
- (5) Diekmann, S.; Dickerson, R. E.; Bansal, M.; Calladine, C. R.; Hunter, W. N.; Kennard, O.; Lavery, R.; Nelson, H. C. M.; Olson, W. K.; Saenger, W.; Shakked, Z.; Sklenar, H.; Soumpasis, D. M.; Tung, C.-S.; von Kitzing, E.; Wang, A. H.-J.; Zhurkin, V. B. Definitions and nomenclature of nucleic acid structure parameters. *J. Mol. Biol.* **1989**, *205*, 787–791.
- (6) El Hassan, M. A.; Calladine, C. R. The assessment of the geometry of dinucleotide steps in double-helical DNA: a new local calculation scheme. *J. Mol. Biol.* **1995**, *251*, 648–664.
- (7) Chandrasekaran, R.; Arnott, S. The structures of DNA and RNA helices in oriented fibers. In *Landolt-Börnstein Numerical Data and Functional Relationships in Science and Technology, Group VII/1b, Nucleic Acids*; Saenger, W., Ed.; Springer-Verlag: Berlin, 1989; pp 31–170.
- (8) Olson, W. K.; Gorin, A. A.; Lu, X.-J.; Hock, L. M.; Zhurkin, V. B. DNA sequence-dependent deformability deduced from protein-DNA crystal complexes. *Proc. Natl. Acad. Sci., U.S.A.* **1998**, *95*, 11163–11168.
- (9) Olson, W. K.; Marky, N. L.; Jernigan, R. L.; Zhurkin, V. B. Influence of fluctuations on DNA curvature. A comparison of flexible and static wedge models of intrinsically bent DNA. *J. Mol. Biol.* **1993**, *232*, 530–554.
- (10) Kratky, O.; Porod, G. Röntgenuntersuchung Gelöster Fadenmoleküle. *Rec. Trav. Chim.* **1949**, *68*, 1106–1122.
- (11) Shore, D.; Baldwin, R. L. Energetics of DNA twisting. I. Relation between twist and cyclization probability. *J. Mol. Biol.* **1983**, *170*, 957–981.
- (12) Horowitz, D. S.; Wang, J. C. Torsional rigidity of DNA and length dependence of the free energy of DNA supercoiling. *J. Mol. Biol.* **1984**, *173*, 75–91.
- (13) Frank-Kamenetskii, M. D.; Lukashin, A. V.; Anshelevich, V. V.; Vologodskii, A. V. Torsional and bending rigidity of the double helix from data on small DNA rings. *J. Biomol. Struct. Dynam.* **1985**, *2*, 1005–1012.
- (14) Coleman, B. D.; Lembo, M.; Tobias, I. A new class of flexure-free torsional vibrations of annular rods. *Meccanica* **1996**, *31*, 565–575.
- (15) Tobias, I. A theory of thermal fluctuations in DNA miniplasmids. *Biophys. J.* **1998**, *74*, 2545–2553.
- (16) Song, L. U.; Schurr, J. M. Dynamic bending rigidity of DNA. *Biopolymers* **1990**, *30*, 229–237.
- (17) Okonogi, T. M.; Alley, S. C.; Reese, A. W.; Hopkins, P. B.; Robinson, B. H. Sequence-dependent dynamics of duplex DNA: the applicability of a dinucleotide model. *Biophys. J.* **2002**, *83*, 3446–3459.
- (18) Braun, W.; Yoshioki, S.; Gō, N. Formulation of static and dynamic conformational energy analysis of biopolymer systems consisting of two or more molecules. *J. Phys. Soc. Jpn.* **1984**, *53*, 3269–3275.
- (19) Higo, J.; Seno, Y.; Gō, N. Formulation of static and dynamic conformational energy analysis of biopolymer systems consisting of two or more molecules—avoiding a singularity in the previous method. *J. Phys. Soc. Jpn.* **1985**, *54*, 4053–4058.
- (20) Olson, W. K.; Bansal, M.; Burley, S. K.; Dickerson, R. E.; Gerstein, M.; Harvey, S. C.; Heinemann, U.; Lu, X.-J.; Neidle, S.; Shakked, Z.; Sklenar, H.; Suzuki, M.; Tung, C.-S.; Westhof, E.; Wolberger, C.; Berman, H. M. A standard reference frame for the description of nucleic acid base-pair geometry. *J. Mol. Biol.* **2001**, *313*, 229–237.
- (21) Wang, J. C. Variation of the average rotation angle of the DNA helix and the superhelical turns of closed cyclic lambda DNA. *J. Mol. Biol.* **1969**, *43*, 25–39.
- (22) Depew, R. E.; Wang, J. C. Conformational fluctuations of DNA helix. *Proc. Natl. Acad. Sci., U.S.A.* **1975**, *72*, 4275–4279.
- (23) Anderson, P.; Bauer, W. Supercoiling in closed circular DNA: dependence upon ion type and concentration. *Biochemistry* **1978**, *17*, 594–600.
- (24) Landau, L. D.; Lifshitz, L. M. *Theory of Elasticity*; Pergamon Press: Oxford, 1986; Chapter 2.
- (25) Coleman, B. D.; Olson, W. K.; Swigon, D. Theory of sequence-dependent DNA elasticity. *J. Chem. Phys.* **2003**, *118*, 7127–7140.
- (26) Olson, W. K.; Swigon, D.; Coleman, B. D. Implications of the dependence of the elastic properties of DNA on nucleotide sequence. *Philos. Trans. R. Soc.* **2004**, *362*, 1403–1422.
- (27) Namoradze, N. Z.; Goryunov, A. N.; Birshtein, T. M. On conformations of the superhelix structure. *Biophys. Chem.* **1977**, *7*, 59–70.
- (28) Levitt, M. How many base-pairs per turn does DNA have in solution and in chromatin? Some theoretical calculations. *Proc. Natl. Acad. Sci., U.S.A.* **1978**, *75*, 640–644.
- (29) Sussman, J. L.; Trifonov, E. N. Possibility of nonkinked packing of DNA in chromatin. *Proc. Natl. Acad. Sci., U.S.A.* **1978**, *75*, 103–107.
- (30) Tobias, I.; Coleman, B. D.; Lembo, M. A class of exact dynamical solutions in the elastic rod model of DNA with implications for the theory of fluctuations in the torsional

- motion of plasmids. *J. Chem. Phys.* **1996**, *105*, 2517–2526.
- (31) Matsumoto, A.; Gō, N. Dynamic properties of double-stranded DNA by normal mode analysis. *J. Chem. Phys.* **1999**, *110*, 11070–11075.
- (32) Matsumoto, A.; Tobias, I.; Olson, W. K. Normal-mode analysis of circular DNA at the base-pair level. 2. Large-scale configurational transformation of a naturally curved molecule. **2005**, *1*, 130–142.
- (33) Kraulis, P. J. MolScript: a program to produce both detailed and schematic plots of protein structures. *J. Appl. Crystallogr.* **1991**, *24*, 946–950.

CT049950R